RESEARCH ARTICLE

A Nonhuman Primate PET Study: Measurement of Brain PDE4 Occupancy by Roflumilast Using (R)-[11C]Rolipram

Akihiro Takano,[1] Tolga Uz,[2] Jesus Garcia-Segovia,[3,4] Max Tsai,[2,5] Gezim Lahu,[2] Nahid Amini,[1] Ryuji Nakao,[1] Zhisheng Jia,[1] Christer Halldin[1]

[1]*Department of Clinical Neuroscience, Center for Psychiatric Research, Karolinska Institutet, Stockholm, Sweden*
[2]*Takeda Development Center Americas, Inc., Deerfield, IL, 60015, USA*
[3]*Takeda Development Center, London, UK*
[4]*Orchard Therapeuitcs, Birchin Lane, London, UK*
[5]*Eli Lilly and Company, Indianapolis, IN, USA*

Abstract

Purpose: Phosphodiesterase 4 (PDE4) inhibition in the brain has been reported to improve cognitive function in animal models. Therefore, PDE4 inhibitors are one of key targets potential for drug development. Investigation of brain PDE4 occupancy would help to understand the effects of PDE4 inhibition to cognitive functions. Roflumilast is a selective phosphodiesterase type 4 (PDE4) inhibitor used clinically for severe chronic obstructive pulmonary disease, but the effects to the brain have not been well investigated. In this study, we aimed to investigate whether roflumilast entered the brain and occupied PDE4 in nonhuman primates.

Procedures: Positron emission tomography (PET) measurements with (R)-[11C]rolipram were performed at baseline and after intravenous (i.v.) administration of roflumilast (3.6 to 200 μg/kg) in three female rhesus monkeys. Arterial blood samples were taken to obtain the input function. Protein binding was measured to obtain the free fraction (fp) of the radioligand. Total distribution volume (V_T) and V_T/fp were calculated as outcome measures from two tissue compartment model. Lassen plot approach was taken to estimate the target occupancy.

Results: The brain uptake of (R)-[11C]rolipram decreased after roflumilast administration. PDE 4 occupancy by roflumilast showed dose- and plasma concentration-dependent increase, although PDE4 occupancy did not reach 50 % even after the administration of up to 200 μg/kg of roflumilast, regardless of outcome measures, V_T or V_T/fp.

Conclusions: This PET study showed that the brain PDE4 binding was blocked to a certain extent after i.v. administration of clinical relevant doses of roflumilast in nonhuman primates. Further clinical PET evaluation is needed to understand the relationship between PDE4 inhibition and potential improvement of cognitive function in human subjects.

Key words: PDE4, Roflumilast, PET, Primate

Correspondence to: Akihiro Takano; *e-mail:* akihiro.takano@ki.se

Introduction

The phosphodiesterase enzyme family plays a vital role for degrading cyclic nucleotides (cyclic adenosine monophosphate (cAMP) and cGMP) in the signal transduction pathway in all

cells. Phosphodiesterase 4 (PDE4) is mainly distributed in the immune cells, brain, and cardiovascular tissues [1, 2]. Roflumilast is the first PDE4 inhibitor to be approved for the treatment of severe chronic obstructive pulmonary disease [3]. Apremilast, another registered PDE4 inhibitor, has been introduced for the treatment of skin diseases such as psoriatic arthritis [4, 5].

In regard to the central nervous system (CNS), the inhibition of PDE4 has been reported to have effects in various *in vivo* models of behavior and inflammation [6]. By preventing the cAMP hydrolysis, PDE4 inhibitors are considered to enhance intracellular signal transduction and increase the phosphorylation of cAMP response element-binding protein (CREB), which enhances the transcription of proteins involved in synaptic plasticity and memory formation [7]. Rolipram has been reported to improve cognitive function in animal models of cognitive impairment in neuropsychiatric and neurodegenerative diseases such as schizophrenia and Alzheimer's disease [8–13].

However, the degree of PDE4 inhibition which could be necessary to translate into improvements of cognitive domains has not been fully evaluated *in vivo*. Therefore, it would be helpful for further understanding and development of PDE4 inhibitors to measure brain target occupancy using clinically available PDE4 inhibitors.

In this positron emission tomography (PET) study, we aimed to investigate in nonhuman primates whether roflumilast entered the brain and demonstrated specific target occupancy of PDE4 using (R)-[^{11}C]rolipram, a PET radioligand for PDE4 [14, 15].

Materials and Methods

Preparation of (R)-[^{11}C] Rolipram

(R)-[^{11}C] rolipram was synthesized as previously reported in detail [16]. Shortly, (R)-[^{11}C]rolipram was synthesized by ^{11}C-methylation of (R)-desmethyl-rolipram in acetone by using [^{11}C]methyl triflate. Purification was performed on a reversed phase HPLC. Radiochemical purity of labeled ligand was more than 99 %.

PET Study

Three female rhesus monkeys (mean weight ± SD, 9.5 ± 2.4 kg, age 8.6 ± 0.1 years old) were examined. The monkeys are owned by the Centre for Psychiatry Research, Department of Clinical Neuroscience, Karolinska Institutet, and housed in the Astrid Fagraeus Laboratory of the Swedish Institute for Infectious Disease Control. The study was approved by the Animal Research Ethics Committee of the Swedish Animal Welfare Agency (Northern Stockholm Region) (N 452/11) and was performed according to the relevant guidelines of the Karolinska Institutet ("Guidelines for Planning, Conducting and Documenting Experimental Research" (Dnr 4820/06-600).

To anesthetize the monkeys during the PET experiments, ketamine hydrochloride (approximately 10 mg/kg) was initially administered intramascularily, and, after endotracheal intubation, a mixture of sevoflurane (2–8 %), O_2, and medical air was administered to maintain the anesthesia. The head was immobilized to the PET bed with a fixation device [17].

The HRRT scanner (Siemens) was used to acquire PET data. A 6-min transmission scan using a single Cs-137 source was performed immediately prior to injection of the (R)-[11C]rolipram. PET emission data were acquired for 93 min as list mode just after injection of radioligand (151–178 MBq; specific radioactivity: more than 188 GBq/μmol and injected mass: less than 0. 26 μg). For the reconstruction of PET images, the ordinary Poisson three-dimensional ordered-subset expectation maximization (OSEM) algorithm was used with 10 iterations and 16 subsets, including modeling of the point spread function, after correction for attenuation, random, and scatter. The resolution of the reconstructed PET images was 1.5 mm in full width at half maximum [18]. The frame duration of the PET images was as follows: 10 s × 9, 15 s × 2, 20 s × 3, 30 s × 4, 60 s × 4, 180 s × 4, and 360 s × 12.

Two brain PET measurements were performed, in one day, under the untreated baseline condition, and after intravenous administration of roflumilast, a selective PDE4 inhibitor. Doses of roflumilast were 3.6, 12, 24, 100, and 200 μg/kg. Twelve micrograms per kilogram and 100 μg/kg of roflumilast were administered to monkey 1, 3.6 and 200 μg/kg were administered to monkey 2, and 24 μg/kg was administered to monkey 3. Roflumilast was administered 3 h before the radioligand injection. The duration of the administration was 10 min with syringe pump at the speed of 1 ml/kg. The time between two PET measurements was approximately 4.5 h. The time between two PET measurements with different doses was more than 5 weeks for monkey 1 and monkey 2.

Arterial blood was collected continuously for 3 min using an automated blood-sampling system (ABSS; Allog AB) at a speed of 3 ml/min from arterial catheter in an artery of the lower limb. One arterial blood sample (2 ml) was taken at 5 min before the radioligand injection to measure the protein binding of the radioligand.

To measure the radioactivity in blood and plasma and the fraction of the metabolite, arterial blood samples (1–2 ml) were drawn at 4, 15, 30, 45, 60, and 90 min after the injection of the radioligand.

Venous blood samples were taken at − 1, 10, 20, 40, 65, and 91 min after the radioligand injection to obtain the plasma concentration of roflumilast and a metabolite, N-oxidate roflumilast.

Metabolite Analysis of (R)-[^{11}C]Rolipram

The amount of unchanged (R)-[^{11}C]rolipram and its radioactive metabolites in monkey plasma was measured using a

reversed-phase radio-HPLC method. After centrifugation of blood at 2000×g for 2 min, the plasma was mixed with acetonitrile (1:1.4). Then, the mixture was centrifuged at 2000×g for 4 min, and the supernatant of the mixture was injected into a HPLC system coupled to an online radioactivity detector. The used radio-HPLC system consisted of an interface module (D-7000; Hitachi: Tokyo, Japan), a L-7100 pump (Hitachi), an injector (model 7125, 5.0 ml loop; Rheodyne: Cotati, USA), and an ultraviolet absorption detector (L-7400, 254 nm; Hitachi) in series with a 150TR Packard radioactivity detector (housed in a shield of 50 mm thick lead and equipped with a 550-l flow cell). Chromatographic separation was made on a XBridge C18 column, (50 mm × 10 mm I.D., 2.5 μm + 10 mm × 10 mm I.D., 5 μm; Waters: New England, USA) using gradient elution. Acetonitrile (A) and 20 mM ammonium phosphate (pH 7) (B) were used as the mobile phase at 6.0 ml/min, according to the following program: 0–3.5 min, (A/B) 25:75 → 55:45 v/v; 3.5–4.0 min, (A/B) 55:45 v/v; 4.0–4.1 min, (A/B) 55:45 → 25:75 v/v; 4.1–5.0 min, and (A/B) 25:75 v/v. Peaks for radioactive compounds that were eluted from the column were integrated, and their areas were expressed as a percentage of the sum of the areas detected radioactive compounds (decay-corrected to the time of injection on the HPLC).

Measurement of Free Fraction of (R)-[¹¹C]Rolipram

The free fraction, fp, of (R)-[¹¹C]rolipram in monkey plasma was estimated using an ultrafiltration method. Initially, plasma (500 μl) or phosphate buffered saline solution (500 μl) as a control were mixed with (R)-[11C]rolipram (50 μl, ~1 MBq) and then incubated at room temperature for 10 min. After the incubation, 200 μl portions of the incubation mixtures were pipetted into ultrafiltration tubes (Centrifree YM-30, Millipore). Then, they were centrifuged at 1500×g for 15 min. Radioactivity in equal aliquots (20 μl) of the ultrafiltrate (Cfree) and of the plasma (Ctotal) was counted using a NaI well counter. Each determination was performed in triplicate. The free fraction was then calculated as fp = Cfree / Ctotal, and after the correction for the membrane binding measured with the control samples, the final results were obtained.tpb

MRI Measurements

An MRI system GE 1.5 T Sigma unit (Milwaukee, WI, USA) was used to obtain T1-weighted MR images. A 3-D SPGR protocol with the following settings was used as the T1 sequence: repetition time (TR) 21 ms, flip angle 35°, FOV 12.8, and matrix 256 × 256 × 128, 128 × 1.0 mm slices.

PET Data Analysis

Regions of interest (ROIs) were delineated manually on the putamen, caudate, hippocampus, amygdale, thalamus, pons, frontal cortex, temporal cortex, anterior cingulate cortex, occipital cortex, parietal cortex, and cerebellum on the co-registered MRI/PET images. Regional uptake was expressed as percentage of standard uptake value (%SUV), which equals uptake (MBq/ml)/injected radioactivity (MBq) × body weight (g) × 100.

The total distribution volume (V_T) and V_T/fp of (R)-[¹¹C]rolipram was calculated with two-tissue compartment models using metabolite-corrected plasma input [19, 20]. Because there were no appropriate regions for the reference region, Lassen plot approach was applied for the current data to estimate the target occupancy and the distribution volume (V_{ND}) of free and nonspecifically bound radioligand [21, 22].

The relationship between the target occupancy and the plasma concentration of the drug (roflumilast, N-oxide roflumilast, and the sum of roflumilast and N-oxide roflumilast) was examined using the following hyperbolic function.

$$\text{Occupancy } (\%) = \text{Occ}_{max} \times \text{Cp}/(\text{Kd} + \text{Cp})$$

where Cp is the concentration of the drug, and Kd is the plasma concentration required to produce 50 % of the maximal target occupancy. The area under the curve (AUC) during the 90 min PET measurements divided by the time length of 90 min was used as the plasma level of the drug at the PET measurements.

Occ_{max} was evaluated in two ways. One was *a priori* fixed to 100 % while the other was estimated by fitting data.

Results

Summed PET images at baseline and after administration of 200 μg/kg of roflumilast are shown in Fig. 1. There was high accumulation of the radioligand in the thalamus and striatum (caudate and putamen) and moderate accumulation in the cortex at baseline. After administration of roflumilast, accumulation was decreased in all the brain regions.

Time activity curves of the brain regions at baseline and after administration of 200 μg/kg of roflumilast are shown in Fig. 2. Compared with the baseline, initial brain uptake of (R)-[¹¹C]rolipram was a little higher after administration of roflumilast, but the washout from the brain was faster. For the cerebellum, the peak value was 534 %SUV and the time to decrease to half was approximately 16.5 min at the baseline while the peak value was 585 % SUV and the time to decrease to half was approximately 8 min after roflumilast administration.

The parent fraction of (R)-[¹¹C]rolipram in the plasma decreased to 32.3 ± 6.4 % at 15 min and 14.9 ± 0.1 % at 90 min, and the metabolite rate did not change significantly
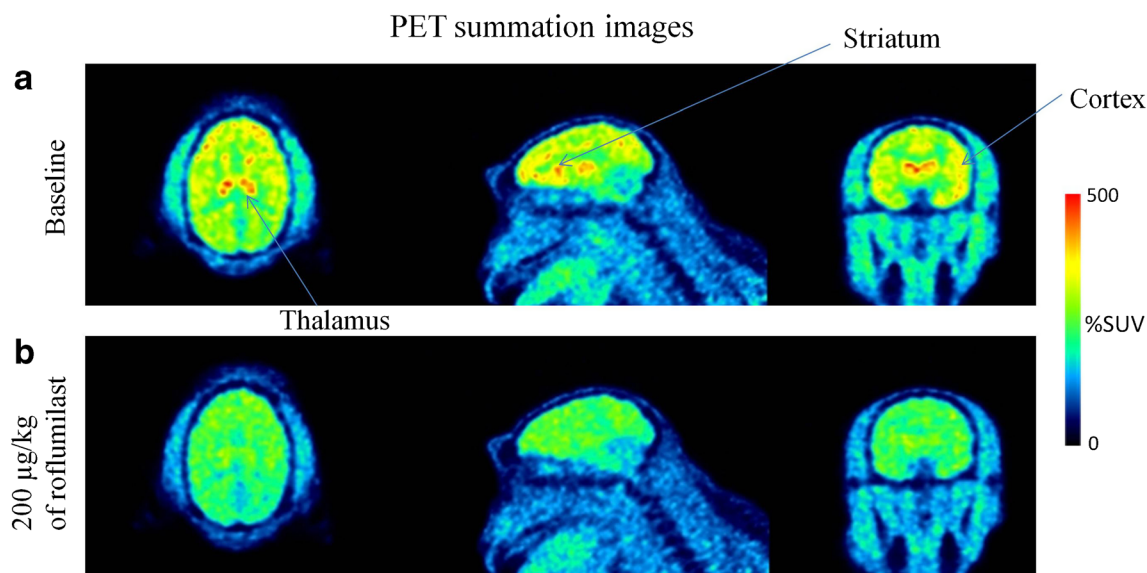
PET summation images

Fig. 1. PET images of (R)-[^{11}C] rolipram summed from 15 to 90 min. **a** Baseline. **b** After administration of 200 μg/kg of roflumilast.

after roflumilast treatment. There were no radioactive metabolites that were more lipophilic than (R)-[^{11}C]rolipram. Free fraction of the radioligand was 39.5 ± 6.0 % at baseline and 44.7 ± 3.6 % after roflumilast administration. There was no correlation between the change of the free fraction and roflumilast concentration.

The calculated V_T and V_T/fp and the percent change of one monkey for whom one baseline PET and post-treatment PET with 200 μg/kg of roflumilast are shown in Table 1. All the brain regions showed the decrease of the V_T and V_T/fp. There was no brain region which can be used as reference region for simplified quantification.
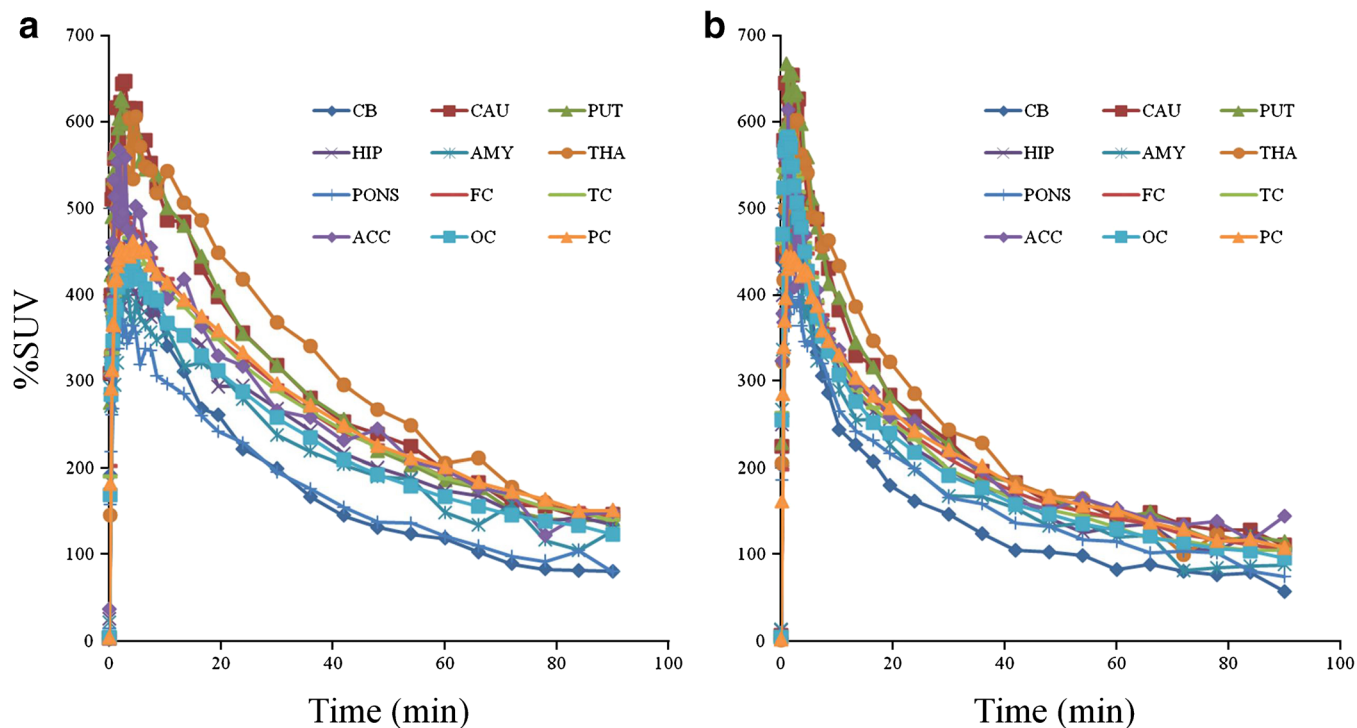

Fig. 2. Brain regional time activity curves of (R)-[^{11}C] rolipram at **a** baseline and **b** after 200 μg of roflumilast. CB cerebellum, CAU caudate, PUT putamen, HIP hippocampus, AMY amygdala, THA; thalamus, FC frontal cortex, TC temporal cortex, ACC anterior cingulated cortex, OC occipital cortex, PC parietal cortex. Percentage of standard uptake value (%SUV) equals uptake (MBq/ml)/injected radioactivity (MBq) × body weight (g) × 100.

Table 1.. V_T and V_T/fp calculated by two tissue compartment model and the percent change in a monkey at the baseline and after 200 μg/kg of roflumilast i.v. administration

	V_T		%change	V_T/fp		%change
	Baseline	Roflumilast		Baseline	Roflumilast	
CB	3.0	2.3	23.8	7.6	5.6	26.5
CAU	5.4	3.9	28.3	13.7	9.5	30.8
PUT	5.0	3.8	24.3	12.7	9.3	26.9
HIP	4.5	3.4	25.2	11.5	8.3	27.7
AMY	4.1	2.8	31.0	10.4	6.9	33.4
THA	5.5	3.7	32.4	13.9	9.1	34.7
PONS	3.0	2.7	11.5	7.7	6.6	14.5
FC	4.9	3.4	30.1	12.4	8.4	32.5
TC	4.9	3.3	32.2	12.3	8.1	34.5
ACC	4.9	3.8	23.7	12.6	9.3	26.4
OC	4.3	3.2	26.2	10.9	7.8	28.8
PC	5.0	3.5	30.4	12.7	8.5	32.8

Lassen plots of PET data after 200 μg/kg of roflumilast administration are shown in Fig. 3. The occupancy at 200 μg/kg of roflumilast was 43.5 % calculated using V_T and 45.5 % calculated using V_T/fp. Estimated PDE4 occupancy and the dose and mean plasma concentration of roflumilast at PET measurements are shown in Table 2. Regardless of the outcome measures of V_T and V_T/fp, PDE4 occupancy was lower than 50 % when up to 200 μg/kg of roflumilast was administered. Plasma concentrations during drug treatment PET measurements for each monkey are shown in Suppl. Fig. 1 (see ESM). The plasma concentrations of roflumilast and N-oxide roflumilast were fairly constant during PET measurements.

The relationship between PDE4 occupancy and the plasma concentration of the drug at the PET measurement is shown in Fig. 4 and Suppl. Fig. 2. The curve fitting was better when the target occupancy was calculated using V_T. Curve fitting was better when maximal occupancy was

estimated by the model than when the occupancy was fixed to 100 %. The estimated K_d values and estimated maximal occupancy are summarized in Table 3. The estimated maximal occupancy was 53.1 to 57.4 %.

Discussion

This PET study showed that roflumilast, a PDE4 inhibitor used for the treatment of COPD, enters the brain and binds to PDE4 in a dose-dependent manner in nonhuman primate brain. However, PDE4 occupancy in the brain was lower than 50 % even when up to 200 μg/kg of rofulmilast was administered.

Roflumilast is the first PDE4 inhibitor to be licensed for the treatment of COPD and was approved in Europe in 2010 and in the USA in 2011 as an oral add-on treatment of COPD. Roflumilast is metabolized principally via the liver into N-oxide roflumilast, which is pharmacologically active with a lower potency but longer half-life than the parent compound [23, 24]. Roflumiast was reported to have no PDE4 subtype selectivity apart from PDE4C while N-oxide rofulmilast has no selectivity for PDE4 subtypes [25]. Therefore, both roflumilast and N-oxide roflumilat have potentials to contribute to PDE4 occupancy.

In this study, roflumilast was administered 3 h before the PET radioligand administration in order to imitate the relationship between roflumilast and N-oxide roflumilast in clinical settings based on internal data (data were not shown).

N-oxide roflumilast was detected under all the drug treatment conditions in this study, and the ratio of the plasma concentration between roflumilast and N-oxide roflumilast was rather constant during PET measurements under all the drug treatment conditions (Suppl. Table 1). Time-dependent different contributions of roflumilast and N-oxide roflumilast to the target binding could not be evaluated due to the constant ratio between them.
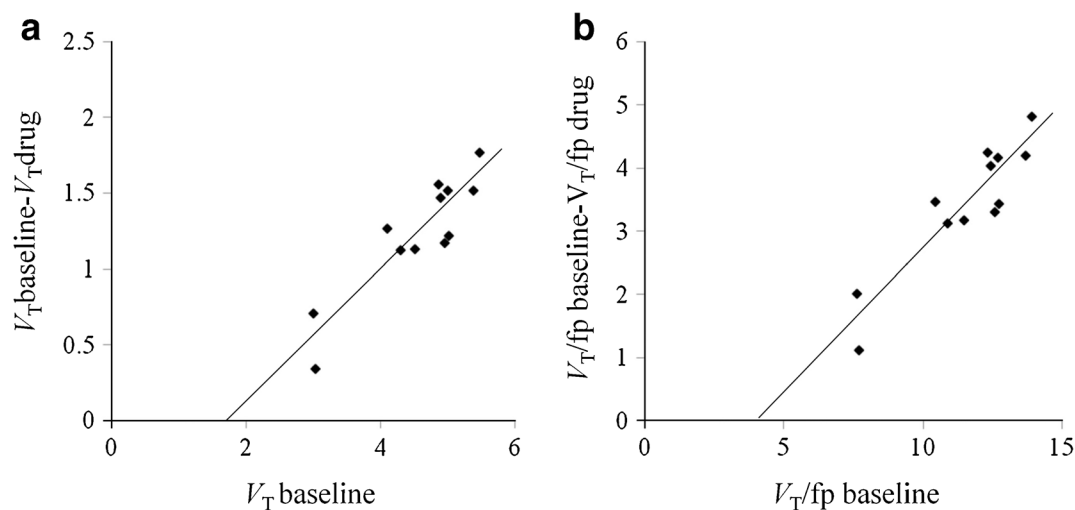

Fig. 3. The occupancy estimation using the Lassen plot. The slope corresponds to the occupancy and the intersection with x axis corresponds to V_{ND}. **a** V_T is used as the outcome measures. The equation of the linear fitting: $Y = 0.4353X - 0.7409$. **b** V_T/fp is used as the outcome measure. The equation of the linear fitting: $Y = 0.4548X - 1.8163$.

Table 2.. PDE4 occupancy by roflumilast calculated with two different outcome measures (V_T and V_T/fp)

Intravenous administration dose of roflumilast (μg/kg)	Mean concentration of roflumilast (ng/ml)	mean concentration of N-oxide roflumilast (ng/ml)	Occupancy (%) using V_T	Occupancy (%) using V_T/fp
200	17.1	57.9	43.5	45.5
100	8.1	24.0	34.7	48.1
24	1.3	4.7	18.5	42.9
12	1.0	1.9	−0.6	5.1
3.6	0.5	0.9	4.5	2.5

In this study, the doses of roflumilast were selected in order to imitate the plasma concentration in the clinical setting. The plasma concentration of roflumilast and N-oxide roflumilast after oral administration of 500 μg of roflumilast, the recommended clinical dose, in human subjects has been reported to be approximately 5 and 9 ng/ml at peak concentration, respectively [23]. As shown in Table 2, the doses up to 200 μg/kg of roflumilast covered the range of the plasma concentration in the clinical settings. Although we have to take into consideration the species difference between the human and NHPs, the estimated PDE4 occupancy of 500 μg of roflumilast would be up to approximately 30–40 % if we apply the human plasma data to the present NHP results of the relationship between the occupancy and the plasma concentration.

The relationship between the target occupancy and plasma concentration suggested that the plotted data fitted better when the maximal occupancy were not fixed as shown in Fig. 4. On the other hand, [³H]rolipram binding was reported to be fully blocked by roflumilast [26]. (R)-[¹¹C]rolipram rat PET study that the brain uptake of (R)-[¹¹C]rolipram was almost completely blocked by cold rolipram [27]. Considering non-PDE4 subtype selectivity of both rolipram and roflumilast [24, 28], full blocking of (R)-[¹¹C]rolipram would be expected by roflumilast

administration. Higher doses of roflumilast than what we tested in this study would be needed to investigate in order to confirm whether *in vivo* maximal target occupancy with (R)-[¹¹C]rolipram can reach 100 % or not.

As outcome measures, V_T and V_T/fp of (R)-[¹¹C]rolipram were calculated in this study because V_T and V_T/fp of (R)-[¹¹C]rolipram were reported to have comparable reproducibility [19], and there was possible change of fp after roflumilast administration. The relationship between the roflumilast and the PDE4 occupancy was weaker when V_T/fp was used to calculate the target occupancy than V_T was used as shown in Fig. 4. In theory, as only free (R)-[¹¹C]rolipram is considered to enter the brain, correction for fp (V_T/fp) should more accurately reflect binding than that without correction (V_T). However, the inclusion of fp in the calculation may introduce additional variability associated with measurement of protein binding. In this study, fp values at the baseline in the same monkeys (monkey 1 and monkey 2) showed rather high variability at different study days (Suppl. Fig. 3). High variability might arrive from technical issues with measurement of protein binding as well as potential physiological conditions in monkeys under anesthesia of induction by ketamine and maintenance by sevoflurane. There was no clear dose-dependent change of fp before and after roflumilast administration although the
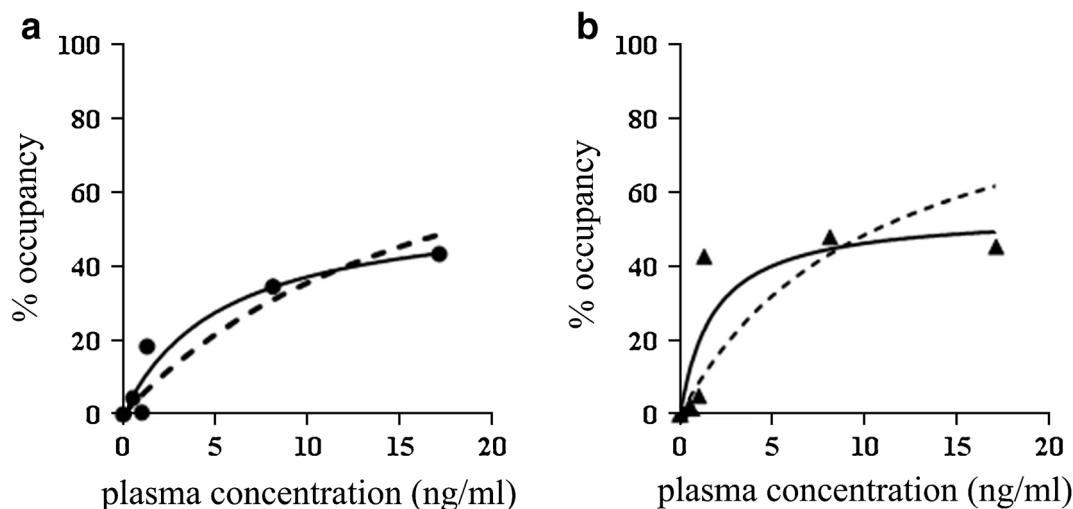

Fig. 4. The relationship between PDE4 occupancy and the plasma concentration of roflumilast. **a** The relationship based on the target occupancy using V_T. **b** The relationship based on the target occupancy using V_T/fp. Dotted lines show the hyperbola where the maximal occupancy was fixed to 100 %. Solid lines show the hyperbola where the maximal occupancy was estimated by the fitting. K_d values and estimated Occ_{max} values are shown in Table 3.

Table 3.. K_d values and estimated $Occu_{max}$ of the plotted data

Drug	V_T		V_T/fp	
	100 % $Occu_{max}$	Estimated Occ_{max}	100 % $Occu_{max}$	Estimated Occ_{max}
Roflumilast	17.9 ng/ml ($R^2 = 0.90$)	5.4 ng/ml ($R^2 = 0.94$), 57.4 %	10.5 ng/ml ($R^2 = 0.53$)	1.8 ng/ml ($R^2 = 0.74$), 54.8 %
N-oxide roflumilast	56.8 ng/ml ($R^2 = 0.89$)	12.6 ng/ml ($R^2 = 0.97$), 53.1 %	31.0 ng/ml ($R^2 = 0.54$)	4.2 ng/ml ($R^2 = 0.85$), 54.0 %
Sum of roflumilast and N-oxide roflumilast	74.8 ng/ml ($R^2 = 0.89$)	17.7 ng/ml ($R^2 = 0.96$), 54.0 %	41.7 ng/ml ($R^2 = 0.53$)	6.0 ng/ml ($R^2 = 0.82$), 54.1 %

Plotted data in Fig. 4 and Suppl. Fig. 2

limited number of the data sets and high variability of fp at the baseline condition might obscure the relation (Suppl. Fig. 3). The target occupancy estimated by V_T/fp was influenced by fp values directly. Considering high variability of fp values at the baseline condition and no clear trend of fp changes before and after roflumilast administration, the target occupancy estimated by V_T/fp would be overestimated or underestimated easily. Therefore, the outcome measures without fp were considered to be more robust in this study.

Compared with other PDE4 inhibitors whose development was stopped due to side effects of nausea and emesis, side effects are typically mild to moderate with roflumilast [29]. Emesis induced by PDE4 inhibitors was reported to be related to the degree of PDE4 inhibition based on the *ex vivo* evaluation of [³H]rolipram binding in the brain although roflumilast was not included in the study [30]. Although species difference is needed to consider, the present study may suggest that 30–40 % of *in vivo* brain PDE4 occupancy, which corresponds to clinical dose of roflumilast, might be an acceptable level of PDE4 inhibition not to induce severe nausea and emesis if the *in vivo* brain target occupancy can be used as an objective parameter. In order to confirm it, direct evaluation between the brain occupancy of PDE4 inhibitors and occurrence of emesis would be necessary in human subjects.

In a recent meta-analysis of roflumilast clinical data [31], 2–5 % of the patients who took roflumiast showed potentially CNS-related side effects such as insomnia, dizziness, and headache. This may support our results of brain penetration of roflumilast.

There has been no clinical data to show the improvement of cognition by PDE4 inhibitors in clinical settings although several lines of research using animal models suggest that PDE4 inhibition could improve some cognitive domains such as executive functions and memory [32, 33]. Regarding PDE4 subtypes, PDE4D is considered to be related to cognitive improvement [34, 35] while PDE4B is also considered to be involved in the cognitive function [36]. It would be worth investigating in future the relationship among treatment with roflumilast, PDE4 occupancy, and effects on cognitive domains in preclinical and clinical settings.

Rolipram binds nonselectively to all PDE4 subtypes (Bruno et al., 2009). As the subtypes differ with respect to their regulatory behavior and tissue expression patterns, PET radioligands with more selective to the subtypes of PDE4 would help to understand the function of PDE4 subtypes in future.

Each dose of roflumilast was investigated only in one monkey. Investigation of the same dose in multiple monkeys would help to evaluate more detailed Kd values.

Conclusions

This PET study showed a certain level of *in vivo* brain PDE4 occupancy after administration of clinically relevant doses of roflumilast, in nonhuman primates. The results would facilitate investigating the relationship between brain PDE4 occupancy and putative procognitive properties of PDE4 inhibitors in human subjects.

Conflict of Interest

References

1. Houslay MD, Sullivan M, Bolger GB (1998) The multienzyme PDE4 cyclic adenosine monophosphate-specific phosphodiesterase family: intracellular targeting, regulation, and selective inhibition by compounds exerting anti-inflammatory and antidepressant actions. Adv Pharmacol 44:225–342. https://doi.org/10.1016/S1054-3589(08)60128-3
2. Tenor H, Hatzelmann A, Church MK, Schudt C, Shute JK (1996) Effects of theophylline and rolipram on leukotriene C4 (LTC4) synthesis and chemotaxis of human eosinophils from normal and atopic subjects. Br J Pharmacol 118(7):1727–1735. https://doi.org/10.1111/j.1476-5381.1996.tb15598.x
3. Giembycz MA, Field SK (2010) Roflumilast: first phosphodiesterase 4 inhibitor approved for treatment of COPD. Drug Des Devel Ther 4:147–158
4. Harrison C (2013) Trial watch: PDE4 inhibitor leads wave of target-specific oral psoriasis drugs. Nat Rev Drug Discov 12(5):335. https://doi.org/10.1038/nrd4017

5. Schafer PH, Day RM (2013) Novel systemic drugs for psoriasis: mechanism of action for apremilast, a specific inhibitor of PDE4. J Am Acad Dermatol 68(6):1041–1042. https://doi.org/10.1016/j.jaad.2012.10.064

6. Martinez A, Gil C (2014) cAMP-specific phosphodiesterase inhibitors: promising drugs for inflammatory and neurological diseases. Expert Opin Ther Pat 24(12):1311–1321. https://doi.org/10.1517/13543776.2014.968127

7. Zhong Y, Zhu Y, He T, Li W, Yan H, Miao Y (2016) Rolipram-induced improvement of cognitive function correlates with changes in hippocampal CREB phosphorylation, BDNF and Arc protein levels. Neurosci Lett 610:171–176. https://doi.org/10.1016/j.neulet.2015.09.023

8. Davis JA, Gould TJ (2005) Rolipram attenuates MK-801-induced deficits in latent inhibition. Behav Neurosci 119(2):595–602. https://doi.org/10.1037/0735-7044.119.2.595

9. Rodefer JS, Saland SK, Eckrich SJ (2012) Selective phosphodiesterase inhibitors improve performance on the ED/ID cognitive task in rats. Neuropharmacology 62(3):1182–1190. https://doi.org/10.1016/j.neuropharm.2011.08.008

10. Imanishi T, Sawa A, Ichimaru Y, Miyashiro M, Kato S, Yamamoto T, Ueki S (1997) Ameliorating effects of rolipram on experimentally induced impairments of learning and memory in rodents. Eur J Pharmacol 321(3):273–278. https://doi.org/10.1016/S0014-2999(96)00969-7

11. DeMarch Z, Giampa C, Patassini S et al (2008) Beneficial effects of rolipram in the R6/2 mouse model of Huntington's disease. Neurobiol Dis 30(3):375–387. https://doi.org/10.1016/j.nbd.2008.02.010

12. Vitolo OV, Sant'Angelo A, Costanzo V, Battaglia F, Arancio O, Shelanski M (2002) Amyloid beta-peptide inhibition of the PKA/CREB pathway and long-term potentiation: reversibility by drugs that enhance cAMP signaling. Proc Natl Acad Sci U S A 99(20):13217–13221. https://doi.org/10.1073/pnas.172504199

13. Rutten K, Basile JL, Prickaerts J, Blokland A, Vivian JA (2008) Selective PDE inhibitors rolipram and sildenafil improve object retrieval performance in adult cynomolgus macaques. Psychopharmacology 196(4):643–648. https://doi.org/10.1007/s00213-007-0999-1

14. DaSilva JN, Lourenco CM, Meyer JH, Hussey D, Potter W, Houle S (2002) Imaging cAMP-specific phosphodiesterase-4 in human brain with R-[^{11}C]rolipram and positron emission tomography. Eur J Nucl Med Mol Imaging 29(12):1680–1683. https://doi.org/10.1007/s00259-002-0950-y

15. Parker CA, Matthews JC, Gunn RN, Martarello L, Cunningham VJ, Dommett D, Knibb ST, Bender D, Jakobsen S, Brown J, Gee AD (2005) Behaviour of [^{11}C]R(-)- and [^{11}C]S(+)-rolipram in vitro and in vivo, and their use as PET radiotracers for the quantificative assay of PDE4. Synapse 55(4):270–279. https://doi.org/10.1002/syn.20114

16. Fujita M, Zoghbi SS, Crescenzo MS, Hong J, Musachio JL, Lu JQ, Liow JS, Seneca N, Tipre DN, Cropley VL, Imaizumi M, Gee AD, Seidel J, Green MV, Pike VW, Innis RB (2005) Quantification of brain phosphodiesterase 4 in rat with (R)-[^{11}C]Rolipram-PET. NeuroImage 26(4):1201–1210. https://doi.org/10.1016/j.neuroimage.2005.03.017

17. Karlsson P, Farde L, Halldin C, Swahn CG, Sedvall G, Foged C, Hansen KT, Skrumsager B (1993) PET examination of [^{11}C]NNC 687 and [^{11}C]NNC 756 as new radioligands for the D1-dopamine receptor. Psychopharmacology 113(2):149–156. https://doi.org/10.1007/BF02245691

18. Varrone A, Sjoholm N, Eriksson L et al (2009) Advancement in PET quantification using 3D-OP-OSEM point spread function reconstruction with the HRRT. Eur J Nucl Med Mol Imaging 36(10):1639–1650. https://doi.org/10.1007/s00259-009-1156-3

19. Zanotti-Fregonara P, Zoghbi SS, Liow JS, Luong E, Boellaard R, Gladding RL, Pike VW, Innis RB, Fujita M (2011) Kinetic analysis in human brain of [^{11}C](R)-rolipram, a positron emission tomographic radioligand to image phosphodiesterase 4: a retest study and use of an image-derived input function. NeuroImage 54(3):1903–1909. https://doi.org/10.1016/j.neuroimage.2010.10.064

20. Zanotti-Fregonara P, Liow JS, Fujita M, Dusch E, Zoghbi SS, Luong E, Boellaard R, Pike VW, Comtat C, Innis RB (2011) Image-derived input function for human brain using high resolution PET imaging with [^{11}C](R)-rolipram and [^{11}C]PBR28. PLoS One 6(2):e17056. https://doi.org/10.1371/journal.pone.0017056

21. Cunningham VJ, Rabiner EA, Slifstein M, Laruelle M, Gunn RN (2010) Measuring drug occupancy in the absence of a reference region: the Lassen plot re-visited. J Cereb Blood Flow Metab 30(1):46–50. https://doi.org/10.1038/jcbfm.2009.190

22. Lassen NA, Bartenstein PA, Lammertsma AA, Prevett MC, Turton DR, Luthra SK, Osman S, Bloomfield PM, Jones T, Patsalos PN, O'Connell MT, Duncan JS, Andersen JV (1995) Benzodiazepine receptor quantification in-vivo in humans using [C-11] flumazenil and pet—application of the steady-state principle. J Cereb Blood Flow Metab 15(1):152–165. https://doi.org/10.1038/jcbfm.1995.17

23. Bethke TD, Bohmer GM, Hermann R et al (2007) Dose-proportional intraindividual single- and repeated-dose pharmacokinetics of roflumilast, an oral, once-daily phosphodiesterase 4 inhibitor. J Clin Pharmacol 47(1):26–36. https://doi.org/10.1177/0091270006294529

24. Hatzelmann A, Morcillo EJ, Lungarella G, Adnot S, Sanjar S, Beume R, Schudt C, Tenor H (2010) The preclinical pharmacology of roflumilast—a selective, oral phosphodiesterase 4 inhibitor in development for chronic obstructive pulmonary disease. Pulm Pharmacol Ther 23(4):235–256. https://doi.org/10.1016/j.pupt.2010.03.011

25. Rabe KF (2011) Update on roflumilast, a phosphodiesterase 4 inhibitor for the treatment of chronic obstructive pulmonary disease. Br J Pharmacol 163(1):53–67. https://doi.org/10.1111/j.1476-5381.2011.01218.x

26. Zhao Y, Zhang HT, O'Donnell JM (2003) Inhibitor binding to type 4 phosphodiesterase (PDE4) assessed using [^{3}H]piclamilast and [^{3}H]rolipram. J Pharmacol Exp Ther 305(2):565–572. https://doi.org/10.1124/jpet.102.047407

27. Itoh T, Abe K, Zoghbi SS, Inoue O, Hong J, Imaizumi M, Pike VW, Innis RB, Fujita M (2009) PET measurement of the in vivo affinity of 11C-(R)-rolipram and the density of its target, phosphodiesterase-4, in the brains of conscious and anesthetized rats. J Nucl Med 50(5):749–756. https://doi.org/10.2967/jnumed.108.058305

28. Bruno O, Romussi A, Spallarossa A, Brullo C, Schenone S, Bondavalli F, Vanthuyne N, Roussel C (2009) New selective phosphodiesterase 4D inhibitors differently acting on long, short, and supershort isoforms. J Med Chem 52(21):6546–6557. https://doi.org/10.1021/jm900977c

29. Oba Y, Lone NA (2013) Efficacy and safety of roflumilast in patients with chronic obstructive pulmonary disease: a systematic review and meta-analysis. Ther Adv Respir Dis 7(1):13–24. https://doi.org/10.1177/1753465812466167

30. Hirose R, Manabe H, Nonaka H, Yanagawa K, Akuta K, Sato S, Ohshima E, Ichimura M (2007) Correlation between emetic effect of phosphodiesterase 4 inhibitors and their occupation of the high-affinity rolipram binding site in Suncus murinus brain. Eur J Pharmacol 573(1-3):93–99. https://doi.org/10.1016/j.ejphar.2007.06.045

31. Garnock-Jones KP (2015) Roflumilast: a review in COPD. Drugs 75(14):1645–1656. https://doi.org/10.1007/s40265-015-0463-1

32. Rutter AR, Poffe A, Cavallini P, Davis TG, Schneck J, Negri M, Vicentini E, Montanari D, Arban R, Gray FA, Davies CH, Wren PB (2014) GSK356278, a potent, selective, brain-penetrant phosphodiesterase 4 inhibitor that demonstrates anxiolytic and cognition-enhancing effects without inducing side effects in preclinical species. J Pharmacol Exp Ther 350(1):153–163. https://doi.org/10.1124/jpet.114.214155

33. Vanmierlo T, Creemers P, Akkerman S, van Duinen M, Sambeth A, de Vry J, Uz T, Blokland A, Prickaerts J (2016) The PDE4 inhibitor roflumilast improves memory in rodents at non-emetic doses. Behav Brain Res 303:26–33. https://doi.org/10.1016/j.bbr.2016.01.031

34. Li YF, Cheng YF, Huang Y, Conti M, Wilson SP, O'Donnell JM, Zhang HT (2011) Phosphodiesterase-4D knock-out and RNA interference-mediated knock-down enhance memory and increase hippocampal neurogenesis via increased cAMP signaling. J Neurosci 31(1):172–183. https://doi.org/10.1523/JNEUROSCI.5236-10.2011

35. Bruno O, Fedele E, Prickaerts J, Parker LA, Canepa E, Brullo C, Cavallero A, Gardella E, Balbi A, Domenicotti C, Bollen E, Gijselaers HJM, Vanmierlo T, Erb K, Limebeer CL, Argellati F, Marinari UM, Pronzato MA, Ricciarelli R (2011) GEBR-7b, a novel PDE4D selective inhibitor that improves memory in rodents at non-emetic doses. Br J Pharmacol 164(8):2054–2063. https://doi.org/10.1111/j.1476-5381.2011.01524.x

36. Titus DJ, Wilson NM, Freund JE, Carballosa MM, Sikah KE, Furones C, Dietrich WD, Gurney ME, Atkins CM (2016) Chronic cognitive dysfunction after traumatic brain injury is improved with a phosphodiesterase 4B inhibitor. J Neurosci 36(27):7095–7108. https://doi.org/10.1523/JNEUROSCI.3212-15.2016